Polyhedron 61 (2013) 143–150

Contents lists available at SciVerse ScienceDirect

Polyhedron

journal homepage: www.elsevier.com/locate/poly

Synthesis, structural and theoretical studies of Pd(II) complexes containing an orthometallated C,C-chelating phosphorus ylide

Kazem Karami [a,*], Mina Salimian [a], Mahboubeh Hosseini-Kharat [a], Giuseppe Bruno [b], Hadi Amiri Rudbari [b], Hossein Tavakol [a]

[a] Department of Chemistry, Isfahan University of Technology, Isfahan 84156/83111, Iran
[b] Dipartimento di Chimica Inorganica, Università di Messina, Vill. S. Agata, Salita Sperone 31, 98166 Messina, Italy

ARTICLE INFO

Article history:
Received 6 April 2013
Accepted 23 May 2013
Available online 7 June 2013

Keywords:
Cyclopalladated
CH bond activation
Phosphorus ylide
Anti-symbiotic effect
Theoretical study

ABSTRACT

The phosphorus ylide $[Ph_3PCHC(O)C_6H_4–NO_2\text{-}4]$ (**1**) reacted with $Pd(OAc)_2$ to give the C,C-orthometallated complexes $[Pd\{\kappa^2(C,C)–C_6H_4PPh_2C(H)CO(C_6H_4–NO_2\text{-}4)\}(\mu\text{-}X)]_2$ (X = Cl (**2**); X = Br (**3**)) as a mixture of isomers, which underwent bridge cleavage reactions with monodentate ligands to afford the monomeric, neutral Pd(II) complexes $[Pd\{\kappa^2(C,C)–C_6H_4PPh_2C(H)CO(C_6H_4–NO_2\text{-}4)\}X(L)]$ (X = Cl, L = Me_3Py (**4**), PPh_3 (**5**); X = Br, L = Me_3Py (**6**), 4-MePy (**7**), PPh_3 (**8**). The complexes were identified and characterized by spectroscopic studies (IR and NMR). The X-ray single crystal analysis of **6** and **7** revealed the presence of an orthometallated C_6H_4-2-PPh_2 unit and a C-linked ylide, Pd—C(H). In the crystal structure of **6**, the location of the Me_3Py ligand is *trans* to the $Pd—C_{ylide}$, according to the anti-symbiotic effect, whereas in **7** the 4-MePy ligand is preferentially *cis* to the $Pd—C_{ylide}$. Density functional theory (DFT) calculations in the reaction solvent (dichloromethane) indicated that the *trans* isomers of **6** and **7** are 3.03 and 0.70 kcal/mol more stable than their *cis* isomers, respectively.

1. Introduction

Phosphorous ylides have been shown to be very versatile ligands due to their ambidentate character. Their coordination occurs with notable selectivity, which has been explained in terms of the anti-symbiotic effect and the nature of the donor atoms bonded to the metal center [1–3]. The utility of metallated phosphorus ylides in synthetic chemistry has been well documented [4,5]. We have recently reported some aspects of the chemistry of α-stabilized keto ylides, which can behave as monodentate and chelate bidentate ligands towards Pd(II), Ag(I) and Hg(II) complexes using different donor atoms [6–10]. Although many bonding modes are possible for keto ylides [11], coordination through carbon is more predominant and is observed with soft metal ions. The orthometallation of phosphorous ylides $R_3P = C(R')(R'')$ (R = alkyl, aryl; R′ and R″ = H, alkyl, aryl, acyl, etc.) [12–21] occurs in the vast majority of cases, regioselectively at the Ph rings of the phosphine unit. With the aim of expanding the scope of this type of orthometallated derivative, and also to gain more insight into their chemical behavior, we have studied the C–H bond activation process, induced by a Pd(II) salt, in ylide **1** (Scheme 1). In addition, we have also studied the reactivity of the resulting orthopalladated complexes towards different neutral ligands.

* Corresponding author. Tel.: +98 3113913239; fax: +98 3113912350.
E-mail address: karami@cc.iut.ac.ir (K. Karami).

0277-5387/$ - see front matter © 2013 Elsevier Ltd. All rights reserved.
http://dx.doi.org/10.1016/j.poly.2013.05.051

2. Results and discussion

2.1. Spectral characterization

Ylide **1** can undergo a C—H activation process at two different positions: (i) the phenyl ring of the phosphine group (Site *A*) and (ii) the phenyl ring of the benzoyl moeity (Site *B*) (Scheme 1). We have recently reported that the exclusive position for palladation on the related ylides $Ph_3P = CHC(O)R$ [6,8] is the phenyl ring bonded to the P atom.

The IR spectrum of **3** shows a strong absorption due to the carbonyl stretching, shifted to higher frequency with respect to the corresponding absorption in the parent ylide **1**, this fact indicating that the ylide is C-bonded to the Pd center [6,8,20–23]. Complex **3** is dinuclear and it is obtained as a mixture of geometric isomers, *cis* (minor) and *trans* (major). This behavior has already been seen for other dinuclear C-coordinated phosphorus ylide complexes [6,20]. In the ^1H and $^{31}P\{^1H\}$ NMR spectra of **3**, two sets of signals are observed for each of the isomers.

The reactivity of complexes **2** and **3** was examined in order to check the stability of the metallated chelating ligand. Thus, the dinuclear complexes **2** and **3** were reacted with neutral monodentate ligands L (L = Me_3Py, 4-MePy and PPh_3) to give the corresponding mononuclear derivatives, $[Pd\{\kappa^2(C,C)–C_6H_4PPh_2C(H)CO(C_6H_4–NO_2\text{-}4)\}X(L)]$ (X = Cl, L = Me_3Py (**4**), PPh_3 (**5**); X = Br, L = Me_3Py (**6**), 4-MePy (**7**), PPh_3 (**8**) (Scheme 1). The spectroscopic

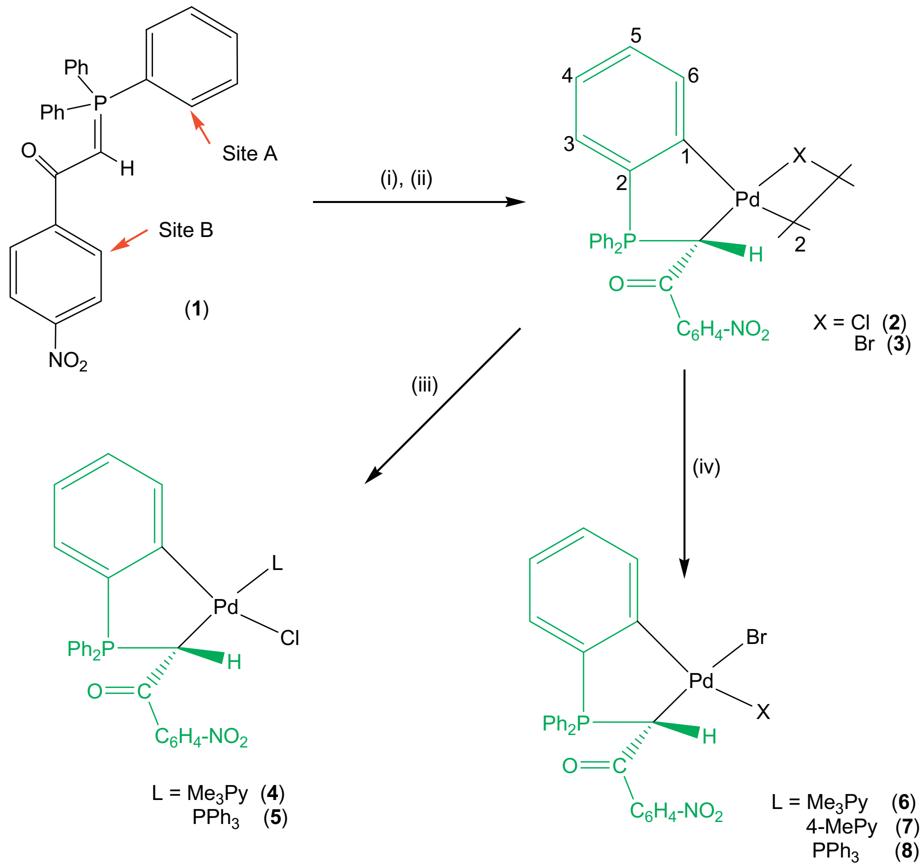

Scheme 1. (i) $Pd(OAc)_2$, CH_2Cl_2, Δ; (ii) KCl or KBr in MeOH; (iii) (complex **2**, CH_2Cl_2, r.t), Me_3Py, PPh_3; (iv) (complex **3**, CH_2Cl_2, r.t), Me_3Py, 4-MePy, PPh_3.

data of **4**–**8** are in accordance with the proposed structure in Scheme 1. In their IR spectra, the band corresponding to ν(CO) appears in the range 1622–1633 cm^{-1}, which is higher than the parent ylide **1**. This high-frequency is a well-established effect in complexes containing other carbonyl-stabilized phosphorus ylides [6,8,20–23] and shows that the ligand coordinates through the carbon atom and not through the oxygen; this has been confirmed for complexes **6** and **7** by X-ray diffraction studies.

In the ^{1}H NMR spectra of **4**–**8**, the $^{2}J_{PH}$ values are smaller than that in the parent ylide; this behavior has already been observed for other C-coordinated carbonyl-stabilized phosphorus ylide complexes [24–26], because the hybridization changes in the ylidic carbon (sp^2 to sp^3) in the C-coordination mode. Moreover, the NMR spectroscopic data show that the mononuclear complexes **4**, **5**, **6** and **8** were obtained as a single isomer, while **7** was obtained as a mixture of the geometric isomers, (a) and (b) depicted in Fig. 1. The ^{1}H NMR spectra of **4** and **6** show signals for the P = C(H) group at 5.23 and 5.34 ppm, whilst the $^{31}P\{^{1}H\}$ NMR spectra show sharp singlets at 19.24 and 21.07 ppm, respectively. The appearance of single signals for the P = C(H) group in each of the ^{1}H and $^{31}P\{^{1}H\}$ NMR spectra indicates the presence of only one isomer [8]. In the ^{1}H NMR spectra, the signals due to the H_6 proton (*ortho* to the metallated position) in **4** and **6** appear at 6.20 and 6.15 ppm, respectively. These signals are clearly shifted to high field with respect to the position in the starting dinuclear derivatives **2** and **3** (δ ~7.12 ppm), and this high-field shift must be due to the anisotropic shielding [27] produced by the pyridine ring of the Me_3Py group, which is non-planar to the phenyl ring. This fact implies a *cis* arrangement of the C_6H_4 fragment of the metallated ligand and the Me_3Py, in accord with the anti-symbiotic behavior of the Pd(II) centre [28].

The ^{1}H, $^{13}C\{^{1}H\}$ and $^{31}P\{^{1}H\}$ NMR spectra of **5** and **8** display a single set of signals in each case, which shows that these complexes are obtained as a single isomer. In the $^{13}C\{^{1}H\}$ NMR spectra of **5** and **8**, the ylidic carbon atoms appear as doublet of doublets at 38.42 and 40.02 ppm, respectively, meaning that each carbon is

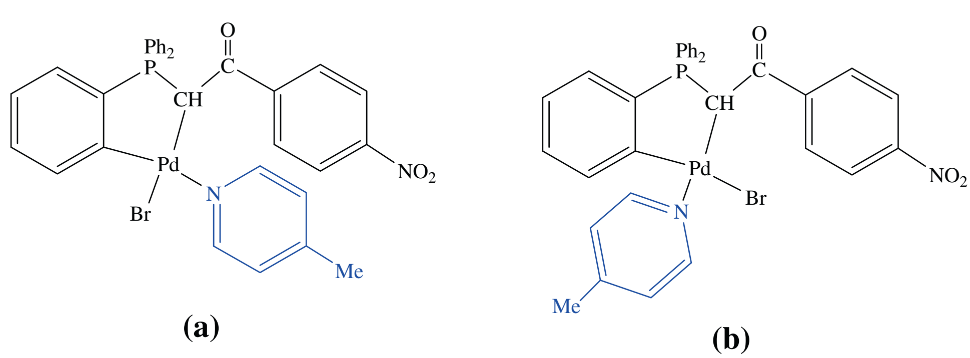

Fig. 1. Possible isomers for complex **7**.

coupled with two different P nuclei (PPh_3 and P = C(H)). Also, the orthometallated carbon atoms (C1) in **5** and **8** appear at 126.23 (d, $^2J_{PC}$ = 11.6 Hz) and 126.33 ppm (d, $^2J_{PC}$ = 11.4 Hz), respectively, coupling with the P atom in the ring, while a coupling with a trans phosphine should give a coupling constant of about 110–130 Hz [29,30]. Moreover, in the ^{1}H NMR spectra, the H_6 proton of the orthometallated C_6H_4 group is shifted to lower frequencies for **5** (6.58 ppm) and **8** (6.60 ppm) because of the anisotropic shielding from the phenyl ring [27,31]. These data support the structure shown in Scheme 1 for **5** and **8**, in which the PPh_3 ligand is *trans* to the ylidic C atom, in good agreement with the *transphobia* between the PPh_3 group and the arylic carbon [20,29,32].

The ^{1}H NMR spectrum of **7** shows two signals for the P = C(H) group that are assigned to a fast equilibrium between the *cis* and *trans* isomers or a dynamic activity for exchange of 4-MePy and Cl groups in solution [1] (Fig. 1).

The major isomer **7a** has been characterized as that containing the 4-MePy ligand *cis* with respect to the ylidic carbon. This assignment of the structures **7a** and **7b** has been carried out by comparison of the chemical shifts of the H_6 proton of the C_6H_4 group (*ortho* to the metallated position) in the two isomers. Thus, the major isomer **7a** shows the signal corresponding to H_6 at δ = 7.02 ppm, while the minor isomer **7b** shows the corresponding signal at δ = 6.52 ppm. This clear upfield shift can be due to the anisotropic shielding undergone by H_6, which is promoted by the *cis* pyridine ligand in **7b**. We have also observed the *cis* structure of complex **7**, with a *cis*-configuration of the coordinated 4-MePy to the carbon (C1) of ylide, in the solid state.

2.2. Crystal structures

Single crystals suitable for structure determinations were obtained by slow evaporation of a concentrated CH_2Cl_2–hexane solution of **6** and **7**, respectively. Crystallographic data and parameters concerning data collection and structure solution and refinement are summarized in Table 1. Figs. 2 and 3 show the ORTEP plot of complexes **6** and **7**, and selected bond distances and angles, respectively. The square planar coordination geometry of the Pd atoms is slightly but not negligibly tetrahedrally distorted, with the metal atoms protruding from the plane of the C_2NBr core by 0.065 and 0.006 Å in **6** and **7**, respectively. The distortion from the regular square planar geometry is indicated by the values of the bond angles subtended at the Pd centers (Figs. 2 and 3).

The P1–C1 bond lengths in **6** and **7** are significantly longer than that observed in the related free ylide (1.711 Å) of the formula $PPh_3C(H)COPh$ [33]. The Pd–C bond distances involving the orthometallated carbon and the ylide carbon atoms in **6** and **7** are not significantly different from those found in related ortho-palladated complexes (1.991(3), 2.017(5) and 2.115 (3), 2.117(5) Å [6]), respectively.

The stabilized resonance structure for the parent ylide is destroyed due to the complexation, thus the C19–C20 and C1–C2 bond lengths (1.435(9) and 1.470(3) Å) in **6** and **7**, respectively, are significantly longer than the corresponding distances found in the similar uncomplexed phosphoranes (1.407(8) Å [34]), meaning that this bond has been relaxed, while the C20–O1 and C2–O1 bond lengths (1.241(8) and 1.221(3) Å in **6** and **7**, respectively) are shorter than that observed in a similar ligand (1.256(2) Å) [34], which indicates that the C-bonding of the ligand fixes the density charge at the C atom and breaks the conjugation.

In the crystal structure of **7**, the PdC_3P five-membered metallacycle assumes an envelope conformation, with the atoms Pd1 and C1 displaced from the mean plane of the remaining four atoms by 0.3995(2) and 0.2556(3) Å.

Comparing **6** and **7**, the crystal structure of **6** shows that the Me_3Py ligand and Pd–C_{ylide} are *trans* to each other, according to the anti-symbiotic effect [28], while in **7** the 4-MePy ligand is *cis* to the Pd–C_{ylide}. A similar behavior was observed earlier in the case of ylide complexes of palladium (II) containing the 4-MePy ligand [8].

2.3. Theoretical studies

2.3.1. Optimized structures

We have attempted to study important aspects of the prepared molecules by computational methods. In this part, two complexes (**6** and **7**) have been investigated. The X-ray structures of these two complexes were also obtained. Therefore, we have optimized the structures of both the *cis* and *trans* (C_{ylide}–Pd–N) isomers of complexes **6** and **7**. The optimized structures of these four molecules are shown in Fig. 4.

According to the the X-ray structures, complexes **6** and **7** have a *trans* and *cis* geometry, respectively. The calculation of the Gibbs free energies of both complexes showed that the *trans* isomers are more stable than the *cis* isomers. The calculated $\Delta G_{cis-trans}$ values for **6** and **7** are 5.96 and 1.54 kcal/mol in the gas phase and 3.03 and 0.70 kcal/mol in the solvent (CH_2Cl_2), respectively. Therefore, since $\Delta G_{cis-trans}$ for complex **7** is very low, its *cis* isomer might be prepared. In addition, we have calculated the dipole moment of these complexes. The calculated dipole moments of complexes $\mathbf{6}_{trans}$, $\mathbf{6}_{cis}$, $\mathbf{7}_{trans}$ and $\mathbf{7}_{cis}$ are respectively 11.58, 12.29, 13.01 and 12.08 Debye. Interestingly, in each complex, the isomer with a lesser dipole moment is the major isomer (*trans* in complex **6** and *cis* in complex **7**). We have not found any reasonable evidence for this observation.

From the optimized structures, molecular parameters can be obtained. The most important parameters for the optimized structures, in comparison with the X-ray parameters, are listed in Table 2. A comparison between the calculated parameters of $\mathbf{6}_{cis}$ and $\mathbf{7}_{trans}$ with those of the X-ray structures confirms that these structures are close to the real structures. In addition, according to the data, in both complexes, the Pd–Br bond length in the *cis* isomer is less than that in the *trans* isomer, and the Pd–N bond length in the *trans* isomer is less than that in the *cis* isomer. This observation shows that the phenyl substituent increases the bond length between the central metal and the opposite ligand, in agreement with a greater *trans* influence of C_{aryl} in relation to C_{ylide}. Moreover, the Br–Pd–N bond angles in the *cis* isomer of both complexes are smaller than in the *trans* isomers.

2.3.2. NBO and population analyses: frontier orbitals and partial charges

We employed population analyses for all the geometric isomers to extract the energies of the frontier molecular orbitals (FMOs). Graphical presentations of the HOMO and LUMO of all the isomers and their energies (eV) are shown in Fig. 5.

Fig. 5 shows noticeable different electron density distributions in the frontier orbitals of the *cis* and *trans* isomers of each complex and the electron density in both the LUMO and HOMO orbitals are different from each other. These differences are related to the location of the electron density and its quantity. Therefore, it is obvious that the reactivity of these complexes is different and the energy values of the frontier orbitals confirm these differences. By comparing the energies of the frontier orbitals, the LUMO–HOMO energy gap in the *cis* isomers are less than that in the *trans* isomers in both complexes, which shows maybe the *cis* isomers are more reactive than *trans* isomers for these two complexes.

NBO calculations are used as a useful method for the determination of many properties, especially for the reproduction of more exact partial atomic charges. The results of these calculations for both isomers of complexes **6** and **7** showed that the carbon atoms

Table 1
X-ray crystallography data.

	6	7
Empirical formula	$C_{34}H_{30}N_2O_3PPdBr$	$C_{32}H_{26}N_2O_3PPdBr$
Formula weight	731.91	703.86
T/K	293	296
Crystal system	monoclinic	monoclinic
Space group	$P2_1/n$	$P2_1/c$
a (Å)	13.0280(2)	10.0671(2)
b (Å)	16.5210(3)	23.2805(5)
c (Å)	15.3470(2)	13.8637(3)
α (°)	90	90
β (°)	108.30(3)	106.782(1)
γ (°)	90	90
V (Å^3)	3136.22	3110.81(11)
Z	4	4
μ (mm^{-1})	1.9538	1.97
D_{calc} (Mg m^{-3})	1.5586	1.563
F (000)	1487	1432
θ Range (°)	2.4–20.12	2.3–26.5
Independent reflections	6236	6789
Data/restraints/parameters	6236/0/379	6789/0/389
Goodness-of-fit (GOF) on F^2	1.03	0.88
Final R indices	R_1 = 0.0641, wR_2 = 0.1498	R_1 = 0.0286, wR_2 = 0.0877
R indices (all data)	R_1 = 0.1162, wR_2 = 0.1755	R_1 = 0.0347, wR_2 = 0.0953

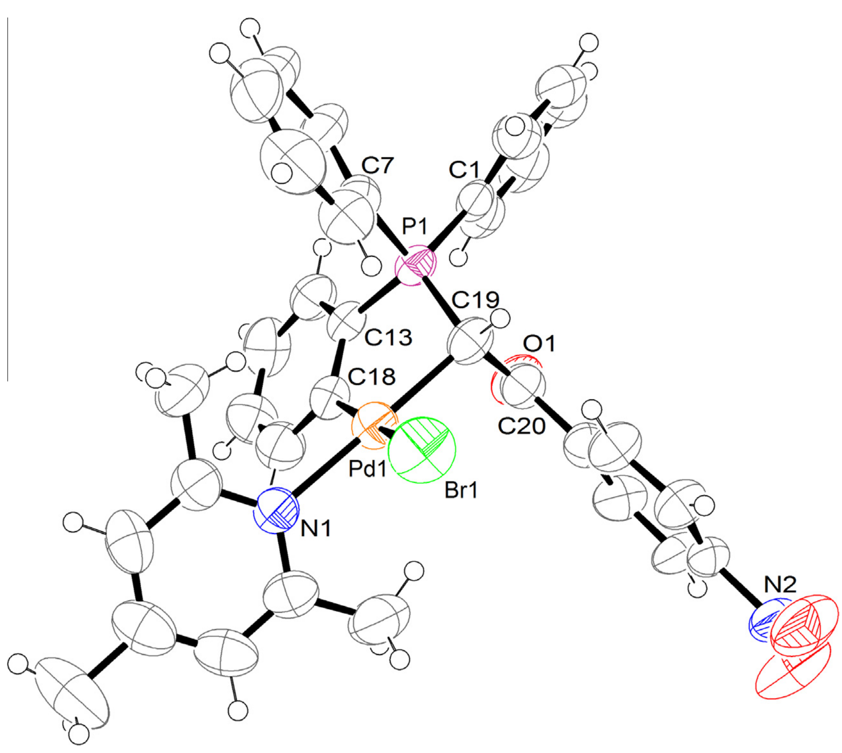

Fig. 2. ORTEP diagram for complex **6** with ellipsoids drawn at the 50% probability level. The hydrogen atoms have been omitted for clarity. Selected bond lengths (Å), and angles (°), Pd1–Br1 2.5345(10), Pd1–N1 2.089(5), P1–C19 1.766(6), P1–C7 1.819(7), P1–C13 1.789(6), P1–C1 1.796(6), C18–Pd1–C19 85.9(3), N1–Pd1–Br1 88.63(15), N1–Pd1–C19 176.0(2), C18–Pd1–Br1 172.72(18), C19–Pd1–Br1 95.38(18), N1–Pd1–Br1 88.63(15).

connected to Pd have different charges in the *cis* and *trans* isomers, while for the other atoms, smaller differences can be observed.

3. Conclusion

New cyclopalladated complexes have been prepared through a C–H bond activation process of the ylide ligand **1**. The palladation is formed selectively at the phenyl ring of the PPh_3 unit (*A* position), giving dinuclear halide-bridge palladacycles **2** and **3**, which are obtained as mixtures of isomers. Neutral monodentate ligands, such as Me_3Py, 4-MePy and PPh_3, split the halide bridging system in **2** and **3** to give mono-nuclear complexes **4**–**8**, in which the five-membered metallacycle remains stable. The reaction is selective in the case of P-ligands, while in the case of N-donors, two isomers were detected in only one case. The crystal structures of **6** and **7** show that the Me_3Py ligand is in a *trans* position to the ylidic carbon, while the 4-MePy ligand is in a *cis* position to this atom. Theoretical calculations in the reaction solvent (dichloromethane) indicate that $\Delta G_{cis-trans}$ in complexes **6** and **7** is 3.03 and 0.70 kcal/mol, respectively.

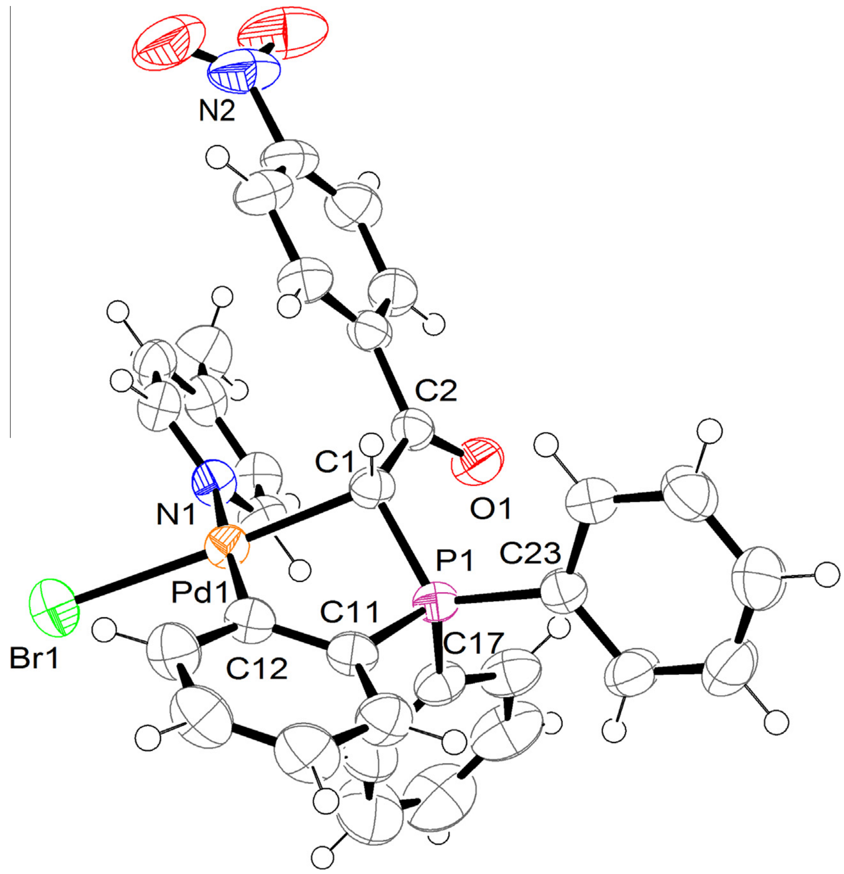

Fig. 3. ORTEP diagram for complex **7** with ellipsoids drawn at the 50% probability level. The hydrogen atoms have been omitted for clarity. Selected bond lengths (Å), and angles (°): Pd1–C12 1.994(2), Pd1–C1 2.116(2), Pd1–Br1 2.4716(4), Pd1–N1 2.126(2), P1–C1 1.775(2), P1–C17 1.807(3), P1–C11 1.781(3), P1–C23 1.800(3), C12–Pd1–C1 83.66(10), N1–Pd1–Br1 88.41(6), C1–Pd1–Br1 174.82(7), C12–Pd1–N1 174.29(10), C1–Pd1–N1 94.66(9), N1–Pd1–Br1 88.41(6).

4. Experimental

4.1. General

The starting materials and solvents were purchased from Merck and were used without further purification. Infrared spectra were recorded on a FT-IR JASCO 680 spectrophotometer in the spectral range 4000–400 cm^{-1} using the KBr pellet technique. NMR spectra were measured on a Bruker spectrometer at 400.13 MHz (^1H), 100.61 MHz (^{13}C) and 161.97 MHz (^{31}P) using standard pulse sequences at 298 K. Melting points were measured on a Gallenhamp 9B 3707 F apparatus. Elemental analysis was performed on a Leco, CHNS-932 apparatus. Ylide **1** and complex **2** were obtained using procedures described earlier [6,35].

4.2. Synthesis of [Pd{κ^2(C,C)–$C_6H_4PPh_2C(H)CO(C_6H_4–NO_2$-4)}(μ-Br)]$_2$ (3)

$Pd(OAc)_2$ (0.0673 g, 0.3 mmol) was added to a solution of **1** (0.1275 g, 0.3 mmol) in CH_2Cl_2 (15 mL) and the resulting mixture was refluxed overnight. The solvent was then evaporated and the resulting deep yellow solid residue was dissolved in MeOH (10 mL) and anhydrous KBr (0.0710 g, 0.6 mmol) was added. A pale yellow solid immediately precipitated. The mixture was stirred for 12 h at room temperature and the resulting suspension was filtered. The pale yellow solid thus obtained was washed with H_2O (5 mL) and Et_2O (15 mL) and air dried to give (**3**). Yield: 0.230 g, 62%. Mp: 208 °C. IR (KBr, cm^{-1}): 1627 ν(CO). ^1H NMR ($CDCl_3$, ppm) δ: 4.96 (br s, 1H, CHP, min.), 5.13 (br s, 1H, CHP, maj.), 7.22–8.11 (m, 36H, H_{Ar}, both); $^{31}P\{^1H\}$ NMR ($CDCl_3$, ppm) δ: 19.51 (s, CHP, min.), 20.08 (s, CHP, maj.). *Anal.* Calc. for $C_{52}H_{38}O_6Br_2P_2N_2Pd_2$: C, 51.13; H, 3.13; N, 2.29. Found: C, 51.20; H, 3.11; N, 2.31%.

4.3. General procedure for the synthesis of [Pd{κ^2(C,C)–$C_6H_4PPh_2C(H)CO(C_6H_4–NO_2$-4)}Cl(L)] (L = Me_3Py (4), PPh_3 (5))

To a suspension of **2** (0.113 g, 0.1 mmol) in dichloromethane (15 mL) was added Me_3Py (0.026 mL, 0.2 mmol) or PPh_3 (0.052 g, 0.2 mmol). The resulting solution was stirred at room temperature for 8 h and then filtered through a plug of $MgSO_4$. The filtrate was concentrated to ca. 2 mL, and *n*-hexane (15 mL) was added to precipitate a deep yellow (**4**) or white (**5**) solid, which was collected and air-dried.

(**4**): Yield: 0.097 g, 71%. Mp: 157 °C. IR (KBr, cm^{-1}): 1622 ν(CO). ^1H NMR ($CDCl_3$, ppm) δ: 2.09 (s, 3H, Me), 2.28 (s, 3H, Me), 2.87 (s, 3H, Me), 5.23 (d, 1H, CHP, $^2J_{PH}$ = 5.5 Hz), 6.20 (d, H_6, C_6H_4, $^3J_{HH}$ = 7.3 Hz), 6.71 (br s, H_5, C_6H_4), 6.93–6.96 (m, 2H, C_6H_4), 7.01–7.18 (m, 1H, Me_3Py), 7.52–7.56 (m, 2H, H_p, PPh_2), 7.62–7.68 (m, 1H, Me_3Py), 7.66–7.71 (m, 4H, H_m, PPh_2), 7.89–7.9 (m, 2H, H_o, PPh_2), 8.21–8.23 (m, 2H, H_o, PPh_2), 8.26–8.28 (d, 2H, H_m, $C_6H_4C(O)$, $^3J_{HH}$ = 8.7 Hz), 8.60–8.61 (d, 2H, H_o, $C_6H_4C(O)$, $^3J_{HH}$ = 8.7 - Hz). $^{31}P\{^1H\}$ NMR ($CDCl_3$, ppm) δ: 19.24 (s, CHP). *Anal.* Calc. for $C_{34}H_{30}O_3ClPN_2Pd$: C, 59.40; H, 4.39; N, 4.07. Found: C, 59.38; H, 4.25; N, 4.12%.

(**5**): Yield: 0.117 g, 70.6%. Mp: 167 °C. IR (KBr, cm^{-1}): 1623 ν(CO). ^1H NMR ($CDCl_3$, ppm) δ: 5.53 (br s, 1H, CHP), 6.58 (d, H_6, C_6H_4, $^3J_{HH}$ = 3.2 Hz), 6.94–6.97 (m, 2H, C_6H_4), 7.19–7.23 (m, 6H, H_m, PPh_3), 7.29–7.35 (m, 7H, 6H_o (PPh_3) + 1H (C_6H_4)), 7.49–7.52 (m, 3H, H_p, PPh_3),7.64–7.64 (m, 2H, H_m, PPh_2), 7.65–7.71 (m, 2H,

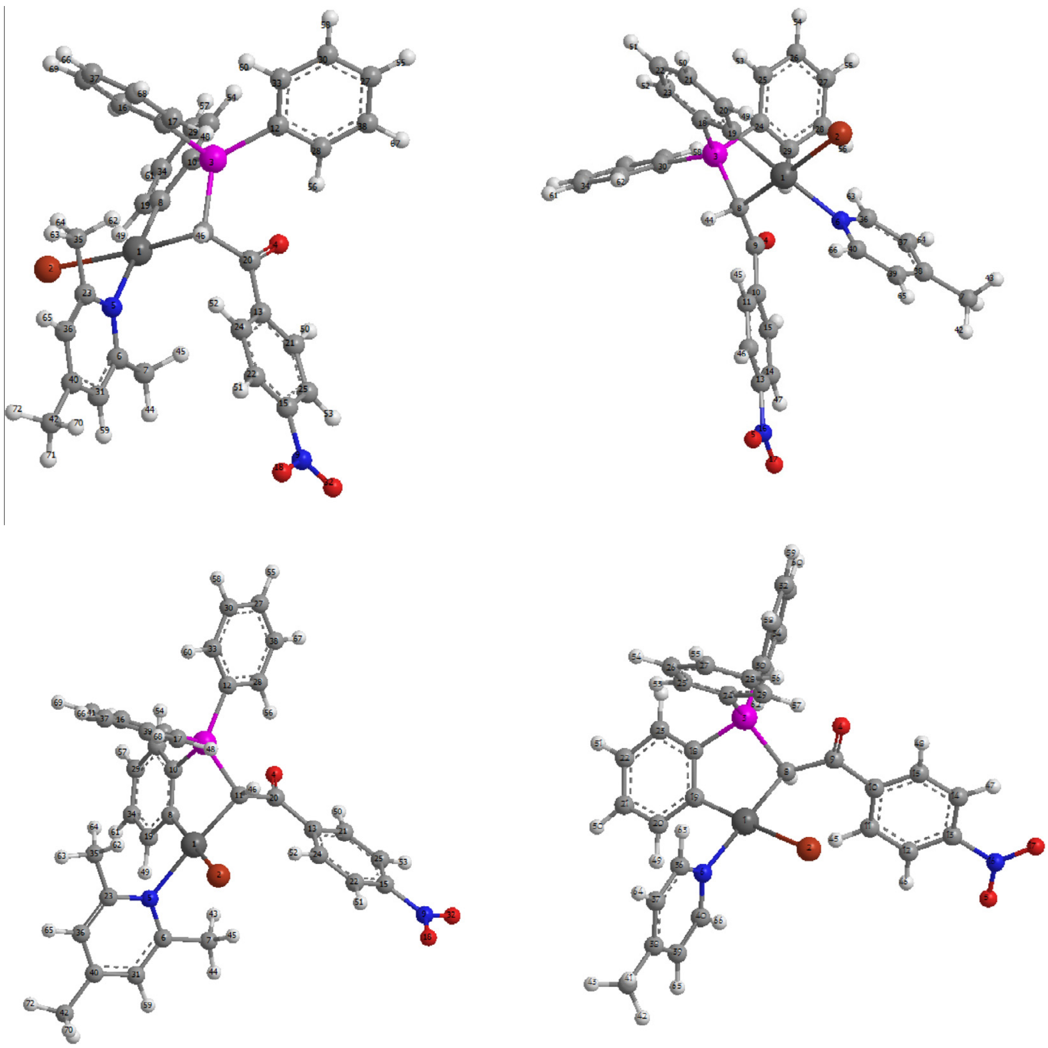

Fig. 4. Graphical presentation of the optimized structures of the *cis* (top) and *trans* (bottom) isomers of complexes **6** (left) and **7** (right).

H_m, PPh_2), 7.71–7.72 (m, 2H, H_p, PPh_2), 7.78–7.91 (m, 2H, H_o, PPh_2), 8.0–8.02 (m, 2H, H_o, PPh_2), 8.21–8.23 (d, 2H, H_m, $C_6H_4C(O)$, $^3J_{HH}$ = 9.2 Hz), 8.56 (d, 2H, H_o, $C_6H_4C(O)$, $^3J_{HH}$ = 8.1 Hz). $^{13}C\{^1H\}$ NMR δ: 38.42 (dd, CHP, $^1J_{PC}$ = 67.7 Hz, $^2J_{PC}$ = 19.5 Hz), $C_{aromatic}$\{123.72 (d, $^1J_{PC}$ = 13.2 Hz), 126.23 (d, C1, $^2J_{PC}$ = 11.6 Hz), 129.08 (d, C_m, PPh_2, $^3J_{PC}$ = 7.1 Hz), 129.68 (d, C_i, PPh_2, $^2J_{PC}$ = 11.3 Hz), 130.26, 130.98, 131.50, 132.84, 134.44, 135.06, 138.14, 140.8, 144.2\}, 132.11 (d, PPh_3, $^3J_{PC}$ = 7.3 Hz), 133.76 (d, C_i PPh_3, $^2J_{PC}$ = 12.3 Hz), 200.21 (CO). $^{31}P\{^1H\}$ NMR ($CDCl_3$, ppm) δ: 15.09 (s, CHP), 32.64 (s, Pd—PPh_3). *Anal.* Calc. for $C_{44}H_{34}O_3ClP_2NPd$: C, 63.78; H, 4.13; N, 1.69. Found: C, 63.81; H, 4.05; N, 1.65%.

*4.4. General procedure for the synthesis of [Pd{κ²(C,C)–C₆H₄PPh₂C(H)CO(C₆H₄–NO₂-4)}Br(L)] (L = Me₃Py (**6**), 4-MePy (**7**), PPh₃ (**8**)*

To a suspension of **3** (0.122 g, 0.1 mmol) in dichloromethane (15 mL) was added Me_3Py (0.026 mL, 0.2 mmol), 4-MePy (0.019 mL, 0.2 mmol) or PPh_3 (0.052 g, 0.2 mmol). The resulting solution was stirred at room temperature for 8 h and then filtered through a plug of $MgSO_4$. The filtrate was concentrated to ca. 2 mL, and *n*-hexane (15 mL) was added to precipitate a deep yellow (**6**), yellow (**7**) or white (**8**) solid, which was collected and air-dried.

6: Yield: 0.107 g, 73%. Mp: 159 °C. IR (KBr, cm^{-1}): 1622 ν(CO). ^1H NMR ($CDCl_3$, ppm) δ: 2.11 (s, 3H, Me), 2.28 (s, 3H, Me), 2.87 (s, 3H, Me), 5.33 (d, 1H, CHP, $^2J_{PH}$ = 5.4 Hz), 6.15 (d, H_6, C_6H_4, $^3J_{HH}$ = 7.6 Hz), 6.73 (s, H_5, C_6H_4), 6.95–6.98 (m, 2H, C_6H_4), 7.17–7.19 (m, 1H, Me_3Py), 7.52–7.56 (m, 2H, H_p, PPh_2), 7.62–7.64 (m, 1H, Me_3Py), 7.67–7.71 (m, 4H, H_m, PPh_2), 7.89–7.93 (m, 2H, H_o, PPh_2), 8.21–8.23 (m, 2H, H_o, PPh_2), 8.26 (dd, 2H, H_m, $C_6H_4C(O)$, $^3J_{HH}$ = 8.8 Hz), 8.25 (dd, 2H, H_o, $C_6H_4C(O)$, $^3J_{HH}$ = 8.8 Hz). $^{13}C\{^1H\}$ NMR δ: 23.92 (Me), 24.81 (Me), 25.00 (Me), 29.94 (CHP), $C_{aromatic}$ \{126.19, 128.30, 129.15, 129.9, 130.25, 130.34, 132.21 (d, $^1J_{PC}$ = 9.6 Hz), 132.82, 133.38 (d, $^2J_{PC}$ = 8.8 Hz), 136.25, 136.76, 141.32\}, 198.13 (CO). $^{31}P\{^1H\}$ NMR ($CDCl_3$, ppm) δ: 21.07 (s, CHP). *Anal.* Calc. for $C_{34}H_{30}O_3BrPN_2Pd$: C, 55.79; H, 4.13; N, 3.82. Found: C, 55.71; H, 4.14; N, 3.80%.

7: Yield: 0.095 g, 68%. Mp: 185 °C. IR (KBr, cm^{-1}): 1633 ν(CO); ^1H NMR ($CDCl_3$, ppm) δ: 2.25 (s, 3H, Me, min), 2.45 (s, 3H, Me, maj.), 5.01 (br s, 1H, CHP, min), 5.30 (br s, 1H,CHP, maj.), 6.52 (m, H_6, C_6H_4, min.), 6.64–6.66 (m, 2H, C_6H_4, min), 6.91–6.97 (m, 2H, C_6H_4, maj.), 7.02 (m, H_6, C_6H_4, maj.), 7.04–7.20 (m, 2H, C_6H_4, both), 7.38–8.62 (m, 36H, PPh_2 + 4-MePy + $C_6H_4C(O)$, both). $^{13}C\{^1H\}$ NMR δ: 20.75, 21.24 (Me, both), 29.94, 32,54 (CHP, both), $C_{aromatic}$ both \{125.48, 126.3, 127.9, 128.1, 129.05, 129.6, 129.8, 129.9, 130.05, 130.74, 133.11 (d, $^3J_{PC}$ = 9.6 Hz), 133.12, 133.38 (d, $^3J_{PC}$ = 8.8 Hz), 136.5, 136.6,141.32\}, 199.4, 201.1 (CO, both). $^{31}P\{^1H\}$ NMR ($CDCl_3$, ppm) δ: 17.25 (s, CHP), 20.43(s, CHP). *Anal.* Calc. for $C_{32}H_{26}O_3BrPN_2Pd$: C, 54.60; H, 3.72; N, 3.98. Found: C, 54.71; H, 3.66; N, 3.92%.

Table 2
Important molecular parameters for the calculated isomers (*trans* and *cis*) in comparison with those from the X-ray structures of **6** and **7**. Bond lengths are in angstroms and bond angles are in degrees.

	Trans	*Cis*	X-ray
Complex **6**			
Bond lengths (Å)			
Pd1–C18	2.06	2.05	2.044(7)
Pd1–C19	2.087	2.116	2.109(7)
Pd1–Br1	2.759	2.719	2.5345(10)
Pd1–N1	2.153	2.197	2.089(5)
P1–C19	2.005	2.003	1.766(6)
P1–C7	1.971	1.967	1.819(7)
P1–C13	1.921	1.909	1.789(6)
Bond angles (°)			
C18–Pd1–C19	87.16	87.65	85.9(3)
N1–Pd1–Br1	86.84	84.01	88.63(15)
N1–Pd1–C19	176.71	94.64	176.0(2)
N1–Pd1–C18	94.86	176.98	90.2(2)
C18–Pd1–Br1	172.07	93.90	172.72(18)
Complex **7**			
Bond lengths (Å)			
Pd1–C12	2.062	2.049	1.994(2)
Pd1–C1	2.086	2.114	2.116(2)
Pd1–Br1	2.733	2.699	2.4716(4)
Pd1–N1	2.127	2.169	2.126(2)
P1–C1	2.002	1.99	1.775(2)
P1–C17	1.961	1.962	1.807(3)
Bond angles (°)			
C12–Pd1–C1	85.365	84.725	83.66(10)
N1–Pd1–Br1	85.506	85.144	88.41(6)
C1–Pd1–Br1	95.07	178.769	174.82(7)
C12–Pd1–N1	94.145	177.697	174.29(10)
C1–Pd1–N1	178.728	96.06	94.66(9)
N1–Pd1–Br1	85.506	85.144	88.41(6)

8: Yield: 0.122 g, 69.6%. Mp: 165 °C. IR (KBr, cm^{-1}): 1623 ν(CO); ^{1}H NMR ($CDCl_3$, ppm) δ: 5.60 (br s, 1H, CHP), 6.60 (m, H_6, C_6H_4, $^{3}J_{HH}$ = 4.6 Hz), 6.96–6.97 (m, 2H, C_6H_4), 7.06–7.08 (m, 1H, C_6H_4), 7.18–7.23 (m, 6H, H_m, PPh_3), 7.29–7.35 (m, 9H, $H_p + H_o$, PPh_3),7.49–7.53 (m, 4H, H_m, PPh_2), 7.63–7.76 (m, 4H, H_o, PPh_2), 7.91–7.98 (m, 2H, H_p, PPh_2), 8.04 (m, 2H, H_m, $C_6H_4C(O)$), 8.21–8.23 (d, 2H, H_o, $C_6H_4C(O)$, $^{3}J_{HH}$ = 8.7 Hz). $^{13}C\{^{1}H\}$ NMR δ: 40.02 (dd, CHP, $^{1}J_{PC}$ = 63.1 Hz, $^{2}J_{PC}$ = 21.0 Hz), $C_{aromatic}${122.32 (d, $^{1}J_{PC}$ = 13.4 Hz), 126.33 (d, C1, $^{2}J_{PC}$ = 11.4 Hz), 128.12 (d, C_m, PPh_2, $^{3}J_{PC}$ = 6.8 Hz), 129.78 (d, C_i, PPh_2, $^{2}J_{PC}$ = 11.6 Hz), 130.06, 130.58, 131.20, 132.74, 134.43, 136.02, 139.12, 140.58, 143.24}, 133.11 (d, PPh_3, $^{3}J_{PC}$ = 8.2 Hz), 135.14 (d, C_i PPh_3, $^{2}J_{PC}$ = 11.8 Hz), 197.4 (CO). $^{31}P\{^{1}H\}$ NMR ($CDCl_3$, ppm) δ: 16.41(s, CHP), 32.74 (s, Pd−PPh_3). *Anal.* Calc. for $C_{44}H_{34}O_3BrP_2NPd$: C, 60.53; H, 3.92; N, 1.60. Found: C, 60.53; H, 4.13; N, 1.60%.

4.5. X-ray structure determinations

Diffraction data for **6** and **7** were measured on a Bruker-Nonius X8 ApexII diffractometer equipped with a CCD area detector by using graphite-monochromated Mo Kα radiation (λ = 0.71073 Å) generated from a sealed tube source. Data were collected and reduced by SMART and SAINT software [36] in the Bruker package. The structures were solved by direct methods [37] and then developed by least squares refinement on F^2 [38,39]. All non-H atoms were placed in calculated positions and refined as isotropic with the "riding-model technique".

4.6. Computational methods

The DFT method was applied to optimize all the structures and to calculate molecular and spectral parameters of the prepared compounds in the gas phase. The energy values in the solvent (dichloromethane) were calculated using SCRF keyword with Tomasi's polarized continuum (PCM) model [40]. The GAUSSIAN 09 program package [41] was employed for optimizing the structures and for the calculation of the molecular properties. To perform DFT calculations, Becke's three-parameter exchange functional [42] was used in combination with the Lee–Yang–Parr correlation functional (B3LYP) with the LANL2DZ basis set [43]. All molecules have been used without any symmetry restriction and C1

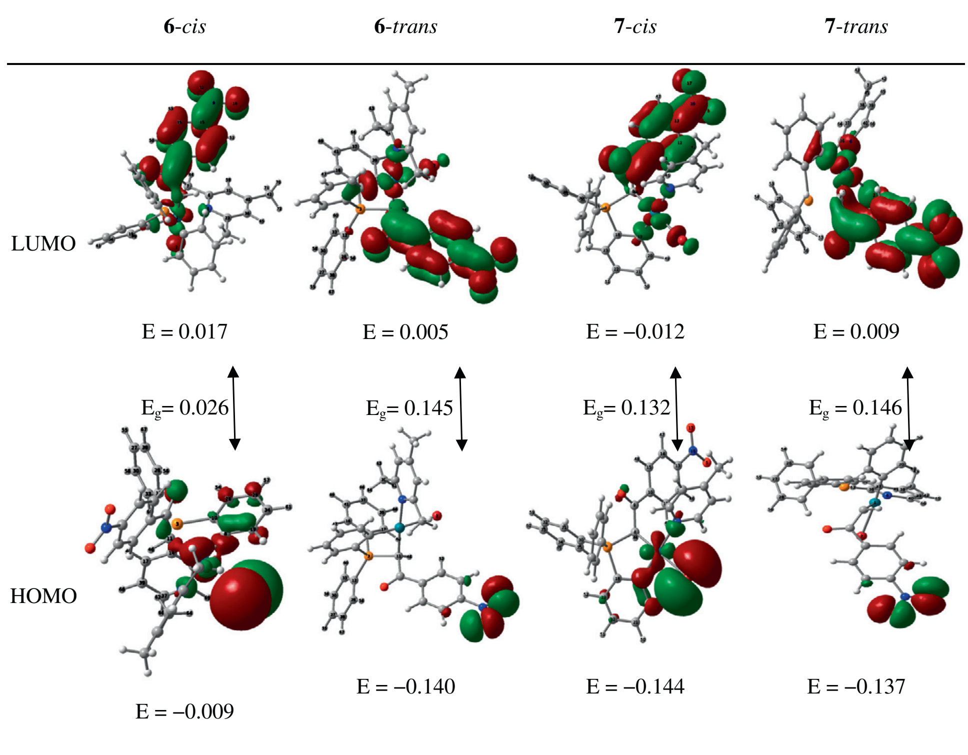

Fig. 5. Graphical presentation of the LUMO and HOMO for the optimized structures of the *cis* and *trans* isomers of complexes **6** and **7**, and their energies (eV).

symmetry was assumed for all molecules. NBO analyses [44] were carried out as implemented in the GAUSSIAN program package using the B3LYP/LANL2DZ level of theory.

Acknowledgement

We are grateful for financial support from the Department of Chemistry, Isfahan University of Technology (IUT).

Appendix A. Supplementary data

CCDC 810769 and 810770 contain the supplementary crystallographic data for compounds **6** and **7**. These data can be obtained free of charge via http://www.ccdc.cam.ac.uk/conts/retrieving.html, or from the Cambridge Crystallographic Data Centre, 12 Union Road, Cambridge CB2 1EZ, UK; fax: +44 1223 336 033; or e-mail: deposit@ccdc.cam.ac.uk.

References

[1] R. Navarro, E.P. Urriolabeitia, J. Chem. Soc., Dalton Trans. (1999) 4111.
[2] E.P. Urriolabeitia, Top. Organomet. Chem. 30 (2010) 15.
[3] A.W. Johnson, W.C. Kaska, K.A.O. Starzewski, D.A. Dixon, Ylides and Imines of Phosphorus, Wiley, New York, 1993.
[4] H.J. Cristau, Chem. Rev. 94 (1994) 1299.
[5] O.I. Kolodiazhnyi, Tetrahedron 52 (1996) 1855.
[6] K. Karami, C. Rizzoli, F. Borzooie, Polyhedron 30 (2011) 778.
[7] K. Karami, O. Buyukgungor, Inorg. Chim. Acta 362 (2009) 2093.
[8] K. Karami, O. Buyukgungor, H. Dalvand, Transition Met. Chem. 35 (2010) 621.
[9] K. Karami, O. Buyukgungor, J. Coord. Chem. 62 (2009) 2949.
[10] K. Karami, O. Buyukgungor, H. Dalvand, J. Korean Chem. Soc. 55 (2011) 38.
[11] J.A. Albanese, A.L. Rheingold, J.L. Burmeister, Inorg. Chim. Acta 150 (1988) 213.
[12] E. Ruba, K. Mereiter, R. Schmid, K. Kirchner, E. Bustelo, M.C. Puerta, P. Valerga, Organometallics 21 (2002) 2912.
[13] J.M. O'Connor, K.D. Bunker, J. Organomet. Chem. 671 (2003) 1.
[14] K. Onitsuka, M. Nishii, Y. Matsushima, S. Takahashi, Organometallics 23 (2004) 5630.
[15] W. Petz, C. Kutschera, B. Neumuller, Organometallics 24 (2005) 5038.
[16] Y. Canac, S. Conejero, M. Soleilhavoup, B. Donnadieu, G. Bertrand, J. Am. Chem. Soc. 128 (2006) 459.
[17] A. Kawachi, T. Yoshioka, Y. Yamamoto, Organometallics 25 (2006) 2390.
[18] E. Serrano, C. Valles, J.J. Carbo, A. Liedos, T. Soler, R. Navarro, E.P. Urriolabeitia, Organometallics 25 (2006) 4653.
[19] K. Karami, C. Rizzoli, M. Mohamadi-Salah, J. Organomet. Chem. 696 (2011) 940.
[20] D. Aguilar, M.A. Aragues, R. Bielsa, E. Serrano, T. Soler, R. Navarro, E.P. Urriolabeitia, J. Organomet. Chem. 693 (2008) 417.
[21] S.J. Sabounchei, H. Nematalab, F. Akhlaghi, H.R. Khavasi, Polyhedron 27 (2008) 3275.
[22] S.J. Sabounchei, S. Samiee, D. Nematollahi, A. Naghipour, D. Morales-Morales, Inorg. Chim. Acta 363 (2010) 3973.
[23] S.M. Sbovata, A. Tassan, G. Facchin, Inorg. Chim. Acta 361 (2008) 3177.
[24] M. Kalyanasundari, K. Panchanatheswaran, W.T. Robinson, H. Wen, J. Organomet. Chem. 491 (1995) 103.
[25] S.J. Sabounchei, A. Dadrass, M. Jafarzadeh, S. Salehzadeh, H.R. Khavasi, J. Organomet. Chem. 692 (2007) 2500.
[26] E.C. Spencer, M.B. Mariyatra, J.A.K. Howard, A.M. Kenwright, K. Panchanatheswaran, J. Organomet. Chem. 692 (2007) 1081.
[27] R. Bielsa, A. Larrea, R. Navarro, T. Soler, E.P. Urriolabeitia, Eur. J. Inorg. Chem. (2005) 1724.
[28] R.G. Pearson, Inorg. Chem. 12 (1973) 712.
[29] L.R. Falvello, S. Fernandez, R. Navarro, A. Rueda, E.P. Urriolabeitia, Organometallics 17 (1998) 5887.
[30] M.W. Avis, K. Vrieze, J.M. Ernsting, C.J. Elsevier, N. Veldman, A.L. Spek, K.V. Katti, C.L. Barnes, Organometallics 15 (1996) 2376.
[31] K. Karami, M. Hosseini Kharat, C. Rizzoli, J. Lipkowski, J. Organomet. Chem. 728 (2013) 16.
[32] J. Vicente, A. Arcas, D. Bautista, J. Organomet. Chem. 663 (2002) 164.
[33] L.R. Falvello, S. Fernandez, R. Navarro, E.P. Urriolabeitia, Inorg. Chem. 38 (1999) 2455.
[34] S.J. Sabounchei, A.R. Dadras, M. Jafarzadeh, H.R. Khavasi, Acta Crystallogr., Sect. E 63 (2007) 3160.
[35] F. Ramırez, S. Dershowitz, J. Org. Chem. 22 (1957) 41.
[36] Bruker AXS Inc., SMART (Version 5.060) and SAINT (Version 6.02), Madison, Wisconsin, USA, 1999.
[37] M.C. Burla, R. Caliandro, M. Camalli, B. Carrozzini, G.L. Cascarano, L. De Caro, C. Giacovazzo, G. Polidori, R. Spagna, J. Appl. Crystallogr. 38 (2005) 381.
[38] G.M. Sheldrick, SHELXL97, Program for Crystal Structure Refinement, University of Göttingen, Germany, 1997.
[39] SHELXT LN, Version 5.10, Bruker Analytical X-ray Inc., Madison, WI USA, 1998.
[40] S. Mietrus, J. Tomasi, Chem. Phys. 65 (1982) 239.
[41] M.J. Frisch, G.W. Trucks, H.B. Schlegel, G.E. Scuseria, M.A. Robb, J.R. Cheeseman, G. Scalmani, V. Barone, B. Mennucci, G.A. Petersson, H. Nakatsuji, M. Caricato, X. Li, H.P. Hratchian, J. Izmaylov, A.F. Bloino, G. Zheng, J.L. Sonnenberg, M. Hada, M. Ehara, K. Toyota, R. Fukuda, J. Hasegawa, M. Ishida, T. Nakajima, Y. Honda, O. Kitao, H. Nakai, T. Vreven, J.A. Montgomery, Jr., J.E. Peralta, F. Ogliaro, M. Bearpark, J.J. Heyd, E. Brothers, K.N. Kudin, V.N. Staroverov, R. Kobayashi, J. Normand, K. Raghavachari, A. Rendell, J.C. Burant, S.S. Iyengar, J. Tomasi, M. Cossi, N. Rega, J.M. Millam, M. Klene, J.E. Knox, J.B. Cross, V. Bakken, C. Adamo, J. Jaramillo, R. Gomperts, R.E. Stratmann, O. Yazyev, A.J. Austin, R. Cammi, C. Pomelli, J.W. Ochterski, R.L. Martin, K. Morokuma, V.G. Zakrzewski, G.A. Voth, P. Salvador, J.J. Dannenberg, S. Dapprich, A.D. Daniels, O. Farkas, J.B. Foresman, J.V. Ortiz, J. Cioslowski, D.J. Fox, Gaussian 09, Revision A.1, Gaussian, Inc., Wallingford, CT, 2009.
[42] A.D. Becke, J. Chem. Phys. 98 (1993) 5648.
[43] C.T. Lee, W.T. Yang, R.G. Parr, Phys. Rev. B 37 (1988) 785.
[44] E.D. Glendening, A.E. Reed, J.E. Carpenter, F. Weinhold, Theoretical Chemistry Institute, University of Wisconsin, Madison, NBO Version 3.1, 1996.